Advances in Concrete Construction, *Vol. 6, No. 4 (2018) 323-344*
DOI: https://doi.org/10.12989/acc.2018.6.4.323

Performance of self-compacting geopolymer concrete with and without GGBFS and steel fiber

Saad Al-Rawi* and Nildem Tayşi[a]

Department of Civil Engineering, Gaziantep University, Gaziantep, Turkey

(Received December 24, 2017, Revised March 30, 2018, Accepted April 4, 2018)

Abstract. The study herein reports the impact of Steel Fiber (SF) and Ground Granulated Blast Furnaces slag (GGBFS) content on the fresh and hardened properties of fly ash (FA) based Self-Compacting Geopolymer Concrete (SCGC). Two series of self-compacting geopolymer concrete (SCGC) were formulated with a constant binder content of 450 kg/m^3 and at an alkaline-to-binder (a/b) ratio of 0.50. Fly ash (FA) was substituted with GGBFS with the replacement levels being 0%, 25%, 50%, 75%, and 100% by weight in each SCGC series. Steel fiber (SF) wasn't employed in the assembly of the initial concrete series whereas, within the second concrete series, an SF combination was achieved by a constant additional level of 1% by volume. Fresh properties of mixtures were through an experiment investigated in terms of slump flow diameter, T50 slump flow time, *V*-funnel flow time, and L-box height ratio. Moreover, the mechanical performance of the SCGCs was evaluated in terms of compressive strength, splitting tensile strength, and fracture toughness. Furthermore, a statistical analysis was applied in order to judge the importance of the experimental parameters, like GGBFS and SF contents. The experimental results indicated that the incorporation of SF had no vital impact on the fresh characteristics of the SCGC mixtures whereas GGBFS aggravated them. However, the incorporation of GGBFS was considerably improved the mechanical properties of SCGCs. Moreover, the incorporation of SF with the total different quantity of GGBFS replacement has considerably increased the mechanical properties of SCGCs, by close to (65%) for the splitting strength and (200%) for compressive strength.

Keywords: Self-Compacting Geopolymer Concrete (SCGC); GGBFS; Steel Fiber (SF); fresh properties; mechanical properties

1. Introduction

Cement is used all over the world in the construction industry due to its ease of working, high strength, and economy. The raw materials used in ordinary Portland cement (OPC) manufacturing are widely abundant, but they also have negative effects on the environment. Despite its wide usage, concrete manufacturing is under observation due to the high emission of carbon dioxide and other greenhouse gases. Approximately 5% of carbon emissions are from the cement industry. The main constituent in ordinary Portland cement manufacturing is hazardous in nature. The high

*Corresponding author, Ph.D. Student, E-mail: sm45139@mail2.gantep.edu.tr
[a]Associate Professor, E-mail: taysi@gantep.edu.tr

http://www.techno-press.org/?journal=acc&subpage=7 ISSN: 2287-5301 (Print), 2287-531X (Online)

carbon emissions found in cement manufacturing is due to the production of carbon dioxide as the main product caused by the reaction and combustion of fossil fuels (Hardjito and Rangan 2005, Rangan 2008).

In order to lessen the environmental effects of cement manufacturing, the struggle for alternative materials must be carried on, which should not only have friendly effects on the environment but also prove to be an effective construction material. In the recent past, huge attempts have been made to reduce the negative effects on the environment from cement manufacturing. The recent contribution of these researchers to use an alternative material instead of ordinary Portland cement is the use of geopolymer concrete (Kong and Sanjayan 2008, Temuujin *et al.* 2010).

Due to its amazing and environment-friendly properties, geopolymer could be called the cement of the future. The use of geopolymer cement as a replacement for ordinary Portland cement has caught attention due to its low yield of carbon emission and better binding properties (Davidovits 1991, Duxson *et al.* 2007, Temuujin *et al.* 2010). Unlike ordinary Portland cement, geopolymer cement does not require temperature for the calcination process, thus saving the natural resources as well as have a low carbon emission. It has been noted that geopolymer cement emits 5 to 6 times less carbon dioxide than the ordinary Portland cement, and that it also encourages the use of by-products of alumina-silicate (Davidovits 1993, Davidovits 2008). Due to these properties, researchers are confident in using geopolymer cement as a replacement for ordinary Portland cement (Hardjito *et al.* 2004).

Self-compacting geopolymer concrete, as the name indicates, has a self-compacting property as well as the fact that it is made with geopolymer cement. The advantages of both are self-compaction and the use of geopolymer cement are combined with this type of concrete (Memon *et al*. 2011, Noushini and Castel 2016). Collected works show that very few attempts have been made on self-compacting geopolymer concrete. The aim of this research is to explore the latency and viability of self-compacting concrete made with the constituents that are locally available. A thorough study of the mechanical and physical properties of the self-compacting geopolymer concrete will be discussed.

The problem with the self-compacting concrete is that it has little cracking resistance, low tensile strength, and limited ductility. Although, these curbs can be eliminated by the addition of fibers (Ganesan and Santhakumar 2013, Tamil and Thandavamoorthy 2014). Fibers can improve the concrete structure's ductile character by possibly increasing the post-cracking energy absorption. Addition of steel fibers also contributes to the low cost as compared to the ordinary self-compacting concrete (Gencel *et al.* 2011, Khaloo *et al.* 2014, Midhun *et al*. 2018). In normal cases, the self-compacting concrete exhibit a homogenous flow by the addition of steel fibers, and the concrete's flowability is improved. The geometry, size, and content of steel fibers can greatly affect the properties of self-compacting concrete. As such, great care shall be carried out when adding the appropriate steel fibers content (Frazão *et al.* 2015).

Although there are limited literature reviews that examine the effect of including GGBFS, SF on the performance of geopolymer concrete, there are limited (or a lack of) studies related to SCGC. The influence of GGBFS and SFs on fresh properties like slump flow diameter, *V*-funnel flow time, *L*-box height ratio, and T50 flow time, and the mechanical properties such as compressive strength, fracture toughness, and splitting tensile strength were investigated within the study. The obtained outcomes of the investigation can be significant for structures by the complete elimination of ordinary Portland cement (OPC). By eliminating ordinary Portland cement, it will not only contribute to the better performance of concrete but it will also be eco-friendly.

Table 1 Physical properties and chemical composition of FA and GGBFS

Component	CaO	SiO_2	Al_2O_3	Fe_2O_3	MgO	SO_3	K_2O	Na_2O	L.O.I	Specific Gravity	Blaine Fineness (m^2/kg)
Fly ash F (%)	1.60	62.40	21.14	7.85	1.76	0.10	0.7	2.45	2.07	2.29	387
GGBFS (%)	34.19	40.4	10.60	1.28	7.63	0.68	2.4	0.17	2.74	2.30	575

Table 2 Physical properties and sieve analysis of fine and coarse aggregates

Sieve Size (mm)	16	8	4	2	1	0.5	0.25	Fineness Modules	Specific Gravity	Absorption
Fine Aggregate	100	100	95.4	63.3	39.1	28.4	16.4	2.57	2.45	1.5
Coarse Aggregate	100	31.5	1	0.5	0.5	0.5	0.4	5.66	2.72	2.4

2. Experimental program

2.1 Materials

To carry out this investigation, FA and GGBFS were obtained from ISKENDERUN - ADANA - TURKEY. Fine and coarse aggregates, an alkaline solution, SF, superplasticizer, and water were utilized. Table 1 presents the chemical composition of FA and GGBFS.

The alkaline solution for SCGC mixtures is a mixture of sodium silicate (Na_2SiO_3) and sodium hydroxide (NaOH) solutions served as the activator. The chemical compositions of the Na_2SiO_3 solution are (Na_2O=10.6%, SiO_2=26.5% and density=1.39 g/ml at 25℃). In addition, sodium hydroxide (NaOH) in the form of flakes (with 98% purity) were utilized. The alkaline solution was prepared at 24 hours prior to utilization.

For concrete preparation, natural fine aggregates and crushed rock, natural coarse aggregates that satisfy the TS 706 EN 12620-A1 (Ersatz 1990), were used. The maximum coarse aggregate size was 12 mm, and the maximum natural fine aggregate size was 4 mm. The 24-hour absorption capacities of coarse aggregates and natural fine aggregates were 1.5% and 2.4% respectively. The aggregate's sieve analysis and physical characteristics were determined based on ASTM C127 (ASTM C127 2010) and are shown in Table 2.

To boost the ductility and tensile strength of the SCGC, SF was added to it. Hooked end SF, with a specific gravity of 7.8, was used in the experiment. The length of fiber was 30 mm and the aspect ratio was 55 (Khaloo *et al.* 2014, Iqbal *et al.* 2015). Master Glenium 51, which is a commercially available superplasticizer, was used to get the preferred flowability and higher workability of fresh concrete. Master Glenium 51 is a poly-carboxylic, ether-based, water reducing, and high-range second generation super plasticizer concrete admixture (Nuruddin *et al.* 2011, Dubey and Kumar 2012). Furthermore, the extra water, which is different from the water used to prepare the sodium hydroxide solution, was also used.

2.2 Concrete mixture

Two different mixtures of SCGC were prepared. These mixtures were designed in such a way that they would cover a series of different mixture variations having the same total binder content

Table 3 Mix proportion of SCGC

MIX ID.	SF	Binder	FA	GGBFS	Fine aggregate.	Coarse aggregate	Molarity	Super plasticizer	Water
	%	kg/m³	%	%	kg/m³	kg/m³		%	%
S0SF0	0	450	100	0	830.65	723.55	12	5	9
S25SF0			75	25	846.39	737.26			
S50SF0			50	50	862.13	750.97			
S75SF0			25	75	877.87	764.68			
S100SF0			0	100	893.61	778.40			
S0SF1	1		100	0	830.65	723.55			
S25SF1			75	25	846.39	737.26			
S50SF1			50	50	862.13	750.97			
S75SF1			25	75	877.87	764.68			
S100SF1			0	100	893.61	778.40			

of (450 kg/m^3). GGBFS was used to replace the FA at level percentages of 25%, 50%, 75%, and 100% by mass. These replacement levels were assigned for the two series. However, only the second series used a fixed percentage of 1% SF by volume (Corinaldesi and Moriconi 2011). Table 3 shows the details of the mix proportions.

2.3 Specimens preparation, curing condition, and casting

In order to secure constant homogeneity and uniformity in every mixture, the mixing order and duration are the key factors. In the first stage, all the ingredients (i.e., coarse and fine aggregates, FA, and GGBFS) were mixed in the dry condition in the 50-liter capacity concrete mixer for 2.5 minutes. After the dry mixing, a homogeneous mixture of alkaline solution and superplasticizer was added to the aggregates and wet mixing was carried on for a further 3 minutes. To ensure homogeneity, the fresh concrete was hand mixed for 2 to 3 minutes.

The fresh mixture of SCGC was then assessed for the essential workability tests required for characterizing SCGC (Slump flow diameter, *L*-box height ratio, *V*-funnel flow time and T50 slump flow time tests were done with regards to the process provided by the EFNARC committee (EFNARC 2005).

Slump flow value can be used to define a freshly poured mix's flowability in unconfined states. Although it is a delicate test, it can normally be performed for all SCCs. This technique is ordered as the main check of fresh concrete used to identify flowability specifications. Furthermore, a visual inspection during the test may also provide supplementary information regarding the uniformity of each delivery and the resistance of segregation. T50 refers to the elapsed time or the time of the concrete to flow through a diameter equal to 50 cm (EFNARC 2005). Based on the EFNARC specifications, the study identified three identical slump flow classes for the application range. Table 4 shows the upper and lower class limits for fresh properties, as specified in EFNARC. The freshly mixed SCGCs' velocity might be assessed using the slump flow time, T50 flow time, and *V*-funnel flow time. These values are not direct indicators of the viscosity of SCGC. However, they have a relationship to the rate of flow.

The *V*-funnel test procedure can be resumed as follows: The *V*-shaped funnel was filled with fresh concrete then the time required for flow down the concrete from the funnel was recorded as

Table 4 EFNARC classes of slump flow, viscosity, and passing ability of SCC mixes

Slump flow classes		
Classes		Slump flow dia (mm)
Slump flow (SF) 1		550-650
Slump flow (SF) 2		660-750
Slump flow (SF) 3		760-850
Viscosity classes		
Class	T50 (sec)	*V*-funnel time (Sec)
Viscosity (VS1/VF1)	≤2	≤8
Viscosity (VS2/VF2)	>2	9 to 25
Passing ability classes		
Passing ability 1		≥0.8 with two rebar
Passing ability 2		≥0.8 with three rebar

the *V*-funnel flow time. Based on the evaluated T50 cm and *V*-funnel slump flow times, EFNARC has specified two classes of viscosity. Table 4 also provides this classification. On the other hand, the *L*-box test is an indication of the fresh mix's passing ability to flow through narrow openings and confined spaces, like regions of congested reinforcement, without segregation or loss of uniformity, and without causing blocking.

The *L*-box test was utilized to evaluate the volume of fresh SCC flow in a horizontal direction and along the spaces between the smooth vertical reinforcing bars, in addition to measuring the height of concrete beyond the reinforcement. The passing ability classes regarding the *L*-box height ratio test are presented in Table 4.

After SCGC was tested in its fresh state, the specimens for hardened properties were prepared. The fresh concrete was mixed thoroughly by hand before it was poured into moulds of cubes, cylinders, and prisms without undergoing compaction, which means that it will fill all of the molds' spaces through its own weight. Furthermore, the top surface of specimens from each mix was scraped so that the excess material can be removed and a smooth finish is achieved. Cylinder specimens with a dimension of (100 mm×200 mm), cubes specimens (100 mm×100 mm×100 mm), and prisms specimens (100 mm×100 mm×500 mm) were used for splitting tensile strength, compressive strength, and fracture toughness test. The specimens were covered by a plastic stretch for 24 hours after casting. They were then placed in the oven for 48 hours at 70℃. The specimens were taken out from the moulds and placed in room temperature conditions up until test day.

2.4 Testing procedure

SCGC cubic specimens were examined for compressive strength according to ASTM C39 (ASTM C39-2001), and cylindrical specimens for splitting tensile, according to ASTM C496 (ASTM C496-2001), using a universal 3000 kN capacity compression testing machine. The rate of loading was 1.5 kN/s for compressive strength and 1 kN/s for splitting tensile strength. The following equation was used to evaluate the splitting tensile strength

$$f_s = \frac{2p}{\pi h \phi} \tag{1}$$

Where *P*,*h* and ∅ are the maximum load (N), the length of the cylinder (mm) and the diameter (mm)respectively.

A closed-loop 250 kN testing machine was utilized according to the recommendation of RILEM 50-FMC/198 Committee (Recommendation 1985) to estimate the fracture toughness G_f of beam specimens. A linear variable displacement transducer (LVDT) was utilized to evaluate the mid-span displacement of beam specimens. The ratio of the notch to height (*a/w*) for prismatic specimens was 0.4. In order to reduce the effective cross-section to 60×100 mm^2, the notch opened for prismatic test specimens by cutting. In addition, the distance between supports was 400 mm. All prismatic beams were tested using displacement control with a rate of loading 0.02mm/minute. Fracture energy of prismatic specimens was achieved under three-point loading according to RILEM (Recommendation 1985) as follow

$$G_f = \frac{\left(w_o + mg\delta_s\right)}{A_{lig}} \tag{2}$$

Where w_0 is the area under the load-displacement curve (N-m), *m* is the mass of the beam (Kg), *g* is the gravity acceleration (9.81 m/s^2), δ_s is the specific displacement (m) and A_{lig} is the area of the ligament (m^2). The details of the specimens and test set up are indicated in Fig. 1.

The net flexural strength, (f_{flix}), was obtained according to the following equation (Akcay and Tasdemir 2009)

$$f_{flex} = \frac{3P_{\max} S}{2B\left(W-a\right)^2} \tag{3}$$

Where P_{max}, *S*, *B*, *W*, and *a* are the peak load (N), span length (mm), the width of the beam (mm), depth of beam (mm), and depth of the notch (mm) respectively.

The critical stress intensity factor (K_{IC}) was utilized to specify the magnitude of stress concentration in cracks. The (K_{IC}) values were obtained according to Eq. (4) (Peterson 1980).

$$K_{IC} = \frac{3P_{\max} l}{2bd^2}\sqrt{a_0}\left(1.93-3.07A+14.53A^2-25.11A^3+25A^4\right) \tag{4}$$

Where P_{max}, *l*, *b*, *d*, and $a_\circ$ are the peak load, the span of the prism, the width of the prism, the depth of prism, and the depth of the notch respectively, since ($A=a_\circ/d$).

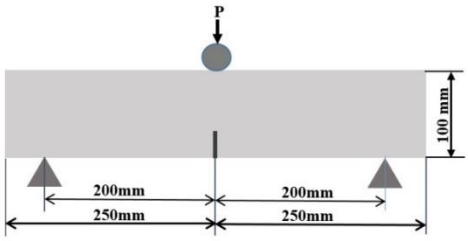

(a) Specimen geometry

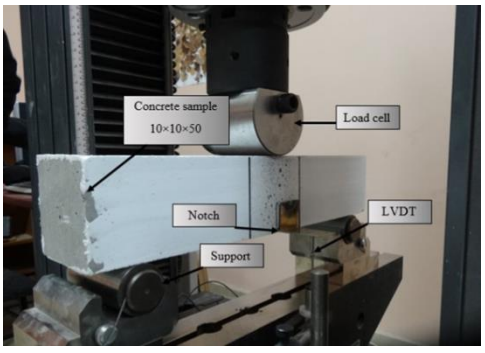

(b) Fracture test mechine

Fig. 1 Specimen geometry and test setup for three-point bending load

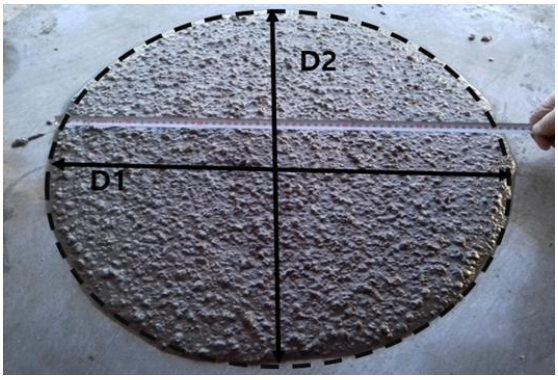

Fig. 2 Measurement of slump flow diameter

3. Experimental results and discussion

3.1 Fresh properties

As self-compacting concrete is known for its stability and filling ability, these properties in the fresh state will be examined through the measurement of its passing ability, flowability, viscosity, and segregation resistance; with each fresh property mentioned previously using one or more techniques (EFNARC 2005).

The flowability of concrete can be approximated by using the slump flow test, whereas viscosity can be determined via the flow times for the T50 slump flow and *V*-funnel flow. In the fresh state, the SCGC requirements that are suitable for a given application may be selected from one or more of the characteristics mentioned above, after the identification by class or target amount as indicated in Table 4 (EFNARC 2005).

Fig. 2 illustrates the typical slump flow diameter measurement. As shown, there was no observed segregation for SCGCs. In addition, to identify the flowability, viscosity, and passing ability of manufactured SCGCs, the slump flow diameter, *V*-funnel flow time, T50 cm slump flow time, and *L*-box height ratio were evaluated.

The outcomes of the fresh properties of the different SCGC mixes having different GGBFS contents are shown in Figs. 3 to 7 and illustrated in Table 5.

It was witnessed from the tests conducted that the replacement of FA by GGBFS by different percentages reduced the fresh properties of SCGC. It was likewise mentioned that the mixes of concrete with the higher percentages of GGBFS were stickier and cohesive. Since low fluidity and flowability of the different SCGC mixtures were observed where higher amounts of GGBFS proportions were used.

Because of its physical properties and chemical characteristics, GGBFS has been reported to be more reactive opposed to FA (Arvaniti *et al*. 2015). Therefore, it was used in this research in combination with fly ash to evaluate its effect on the fresh and hardened properties of SCGC.

Because of the higher surface area and extremely fine particle size, GGBFS increased the water requirement of concrete. As a result, the workability of fresh concrete decreased. This hypothesis became true during this investigation. The addition of GGBFS as a replacement of FA in SCGC resulted in the loss of workability. This might be explained by the increased surface area of GGBFS particles.

Table 5 Fresh properties of SCGC

Mix code	Slump flow (mm)	T50 (sec)	*V* funnel (sec)	*L* box hight ratio
S0SF0	785	2.25	8.02	1
S25SF0	765	2.47	11.5	0.97
S50SF0	730	2.96	13.57	0.92
S75SF0	690	3.56	16.18	0.86
S100SF0	672	4.03	18.05	0.81
S0SF1	755	2.41	9.12	0.97
S25SF1	740	2.68	12	0.93
S50SF1	712.5	3.08	14.09	0.86
S75SF1	680	3.73	17.27	0.81
S100SF1	660	4.12	19.4	0.76

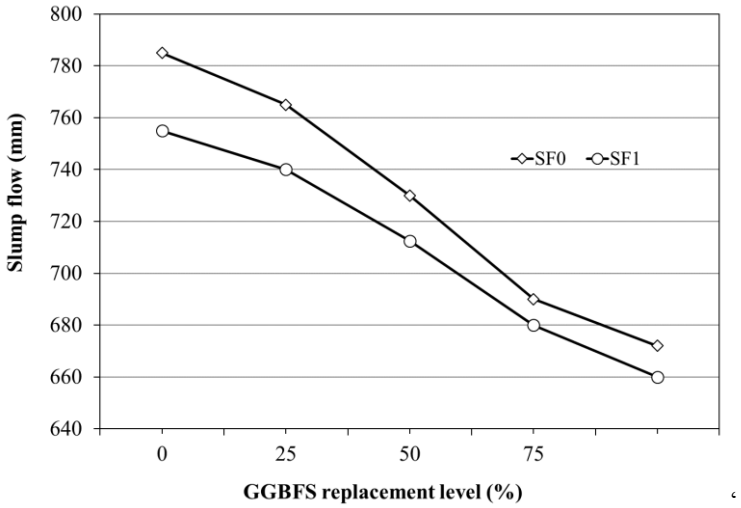

Fig. 3 Effect of GGBFS level and SF on slump diameter values

3.1.1 Effect of GGBFS and SF on slump flow diameter

As shown in Fig. 3, it was observed from the tests that concrete without GGBFS and SF i.e., (S0F0) had the highest slump flow diameter of 785mm. While the lower flow diameter of 672 mm was observed in the mixture having 100% GGBFS replacement (S100SF0). However, the incorporation of SF resulted in a downshift value of slump flow with the similar GGBFS replacement levels. The slump flow amounts of the mixtures containing SFs were varied between 755 and 650 mm. The slump flows for SCGCs of all mixtures (with and without SF) were on the range of (Slump flow 2) class except the control mix which was in the range of (Slump flow 3) class. According to EFNARC (EFNARC 2005), the SCGCs in Slump flow 2 can be used for structures with complex shapes, vertical applications in very congested structures, or for filling under formwork. However, SCGCs in the range of Slump flow 3 exhibit a better surface finish compared to Slump flow 2 when used in normal vertical applications. However, it is more challenging to control segregation resistance.

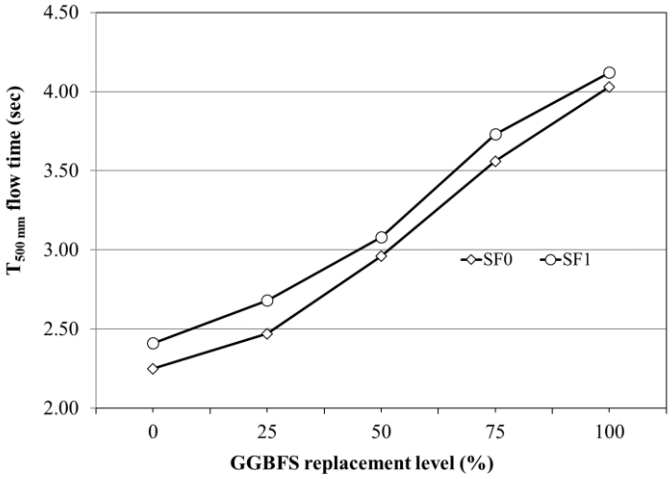

Fig. 4 Effect of GGBFS level and SF on T50 flow time values

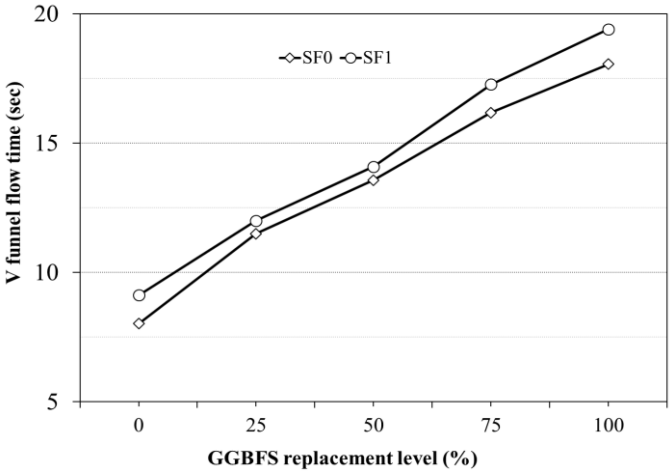

Fig. 5 Effect of GGBFS level and SF on *V*-funnel time values

3.1.2 Effect of GGBFS and SF on slump flow time

Based on the results of T50 cm slump flow time, it was revealed that the replacement values of GGBFS increased the slump flow time and that the SCGC needs more time to get to the 50 cm diameter. However, the incorporation of SF exhibited a systematic increase. Since the T50 cm slump flow time for the overall variation was found to be in the range of 2.25 s to 4.12 s as seen in Fig. 4.

3.1.3 Effect of GGBFS and SF on V funnel flow

The time of *V*-funnel flow is a reflection of the flowability and the viscosity of SCGC. Based on the results, it was seen that the *V*-funnel flow times had a very close behavior to slump flow diameters. In addition, the maximum *V*-funnel flow time (55% and 53%) was observed for the SCGCs mixtures including 100% GGBFS replacement with (1%) SF and without SF respectively,

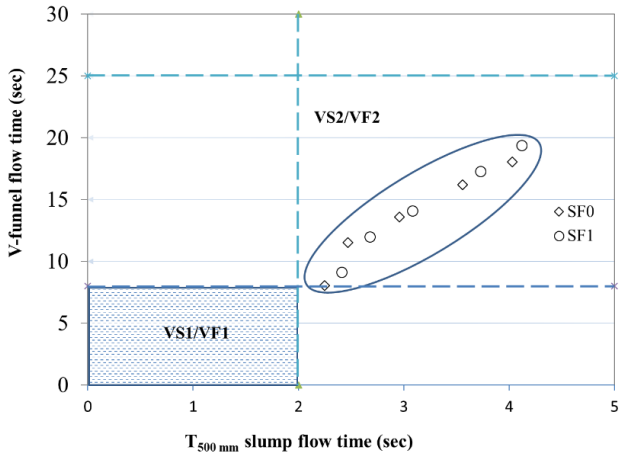

Fig. 6 Variation of viscosity classes with T50 slump flow and *V*-funnel flow time

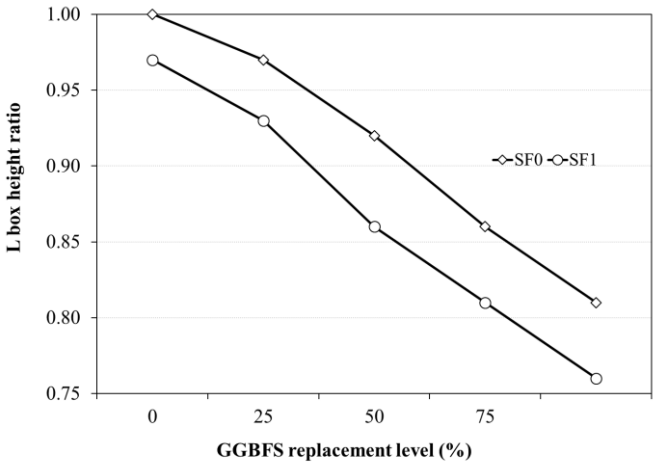

Fig. 7 Effect of GGBFS level and SF on *L*-Box height ratio

as shown in Fig. 5. When taking the interaction of *V*-funnel flow and slump flow times, as indicated in Fig. 6, into account, it was observed that all of the SCGCs mixtures belonged to the boundaries of the viscosity class (VS2/VF2) where (VS2 or VF2) mean the viscocity class as defined in table 4 by the EFNARC. In addition, it was emphasized that such concrete might be helpful in improving segregation resistance or limiting the formwork pressure (EFNARC 2005).

3.1.4 Effect of GGBFS and SF on L-box height

To determine the produced SCGCs' passing ability, the *L*-box height ratio was identified. The test offered the H2/H1 ratio as a way of measuring the passing ability among the reinforcing bars. When movement of concrete has ceased, measure the vertical distance, at the end of the horizontal section of the *L*-box, between the top of the concrete and the top of the horizontal section of the box as H2 mm. The same procedure is used to calculate the depth of concrete immediately behind the gate as H1 mm. Fig. 7 presents the variations within the three bar *L*-box height ratio. The *L*-

box height ratio for a SCC to have the passing ability should be equal to or greater than 0.8. This ratio for the concretes exhibiting perfectly fluid behavior is equal to 1. The results presented in Fig. 7 reveal that all the mixtures met the EFNARC limitation provided for the *L*-box height ratio except the mixtures containing 100% GGBFS and 1% SF. In addition, the *L*-box height ratio decreased with an increase in the GGBFS replacement level. However, the integration of SF with 100% of slag made it possible for the SCGCs to surpass the limitation ratio (less than 0.8).

3.2Hardened properties

3.2.1 Compressive strength

Concrete is considerably recognized for its compressive strength, and it is one of the most vital mechanical properties of concrete. The structure's service life completely relies on the hardened properties of concrete. It was noted that the specimens with 0% GGBFS (100% FA) had to be removed from the molds two or three days after they were cast, since they failed to get the target hardening after one day due to the low amount of CaO in FA which is the main factor affecting the initial setting time of concrete. The addition of GGBFS in FA-based geopolymer concrete accelerated the setting time. The average of the three identical samples was applied to accept the value of the compressive strength of each mix of concrete. Fig. 8 illustrates the influence of the GGBFS content in the matrix.

The compressive strength of SCGC was expressively increased by the addition GGBFS. Furthermore, it was indicated that the compressive strength for the first series of mixtures was arranged between (24.25-76.19) MPa, since the compressive strength of SCGC improved up to more than 200% for (S100SF0) specimens. These results showed the substantial effect that GGBFS has on the compressive strength values of SCGCs mixtures. The lowest compressive strength in FA-based geopolymer concrete specimens were attributed to the low calcium content (Dombrowski and Weil 2007, Belkowitz *et al.* 2015, Jindal *et al.* 2017) and low activity of FA (Chi and Huang 2013, Ç evik *et al.* 2018).

The influence of GGBFS, FA, and GGBFS/FA combinations on compressive strength of OPC and geopolymer concretes were also examined and it was concluded that the compressive strength

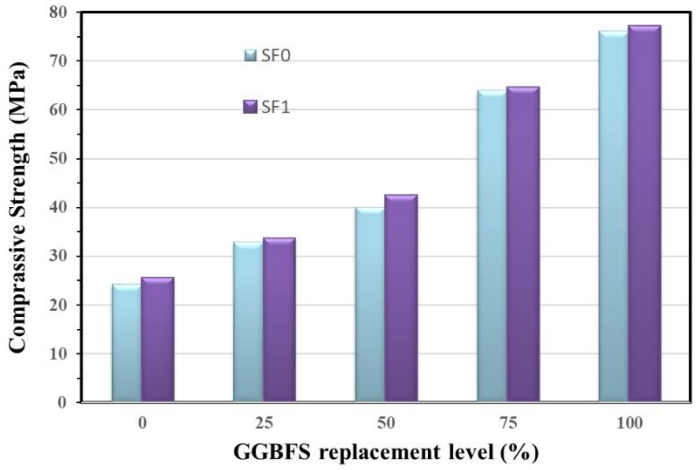

Fig. 8 Effect of GGBFS and SF replacement on compressive strength

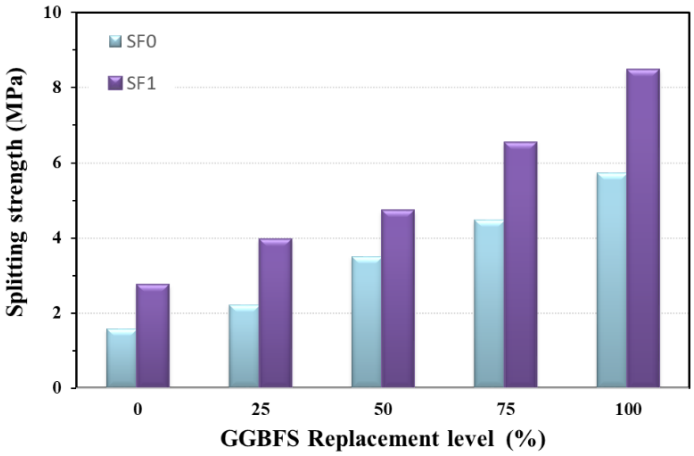

Fig. 9 Effect of GGBFS and SF replacement on splitting strength

of the geopolymer concretes were increased in the order of 100% FA-based GPC< OPC<FA/GGBFS combination GPC<100% GGBFS-based GPC. Less content of reactive calcium was observed after the XRD results on the 100% FA specimens, resulting in the low amount of Calcium Silicate Hydrate (C-S-H) (the main form that is responsible for strength). As a result, a low mechanical performance was obtained for FA-based geopolymer specimens, since the less amount of CaO in the FA did not contribute to the C-S-H creation (Chi and Huang 2013).

As it can be seen from Fig. 8 in the second series, incorporating the SF caused in slightly increasing in the compressive strength of the SCGCs without dependent on the combination of GGBFS replacement. It was recorded that the compressive strengths at the age of 28 days of OPC concrete manufactured with w/b ratio of 0.46 were (41.3, 46.4, and 47.3) MPa for SF volume fractions of (0%, 0.5%, and 1.0%) respectively (Peterson 1980).

3.2.2 Splitting tensile strength

The relationship between the tensile and compressive strength in FA-based SCGC with GGBFS were observed to deliver very close similarities to that of OPC concrete. The increase in the amounts of compressive strength normally caused in a parallel relative increase of the values tensile strengths. Fig. 9 shows the splitting tensile strength test results for the different SCGC mixes with and without SF, with a variable percentage of GGBFS levels. It was indicated that splitting tensile strength values were increased with an increase in GGBFS replacement level when compared with the control mix (100% FA).

In addition, the increase in the amounts of splitting tensile strength that resulted due to the incorporation of GGBFS compared to the control mix (S0SF0) were 40.5%, 121.5%, 226%, and 308% for the mixes S25SF0, S50SF0, S75SF0, and S100SF0 respectively. Moreover, the combination of GGBFS replacement level with the addition of 1% of the SF volume resulted in a superior increase in the splitting tensile strength compared to the control mix without SFs (S0SF0). The increasing amounts were 72.8%, 150%, 261%, 313%, and 423% for the mixes S0SF1, S20SF1, S50SF1, S75SF1 and S100SF1 respectivly. Ganesan and Santhakumar reported that the main objective of the addition of SFs was to increase the tensile strain capacity of the concrete (Ganesan and Santhakumar 2013). Also, it was reported in the literature that tensile strength can

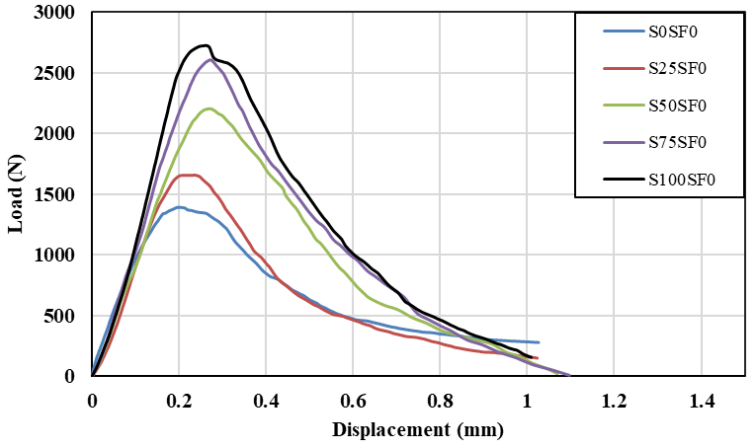

(a) Effect of variance replacement percentage of GGBFS on load displacement

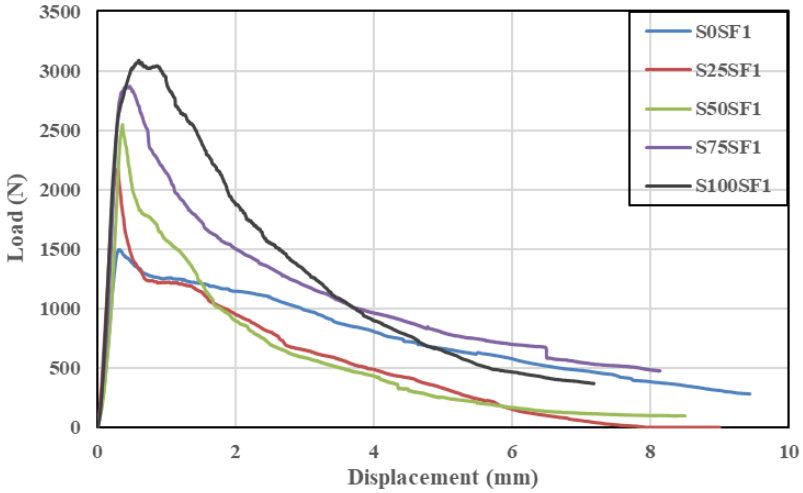

(b) Effect of the combination of SF and GGBFS on load displacement

Fig. 10 Load displacement of SCGCs mixes

significantly increase when fibers were added to the concrete due to the crack arresting effect of the fibers (Belkowitz *et al*. 2015, Gülşan *et al*. 2018, Midhun *et al*. 2018).

3.2.3 Fracture performance

The load-displacement patterns of SCGC at 28 days are presented in Fig. 10, and the results are summarized in Table 6. In general, all SCGC curves exhibited a linear upward slope until load at the first cracking on specimens. During the test process, after the load reaches the peak load, cracks appeared which resulted in a descending curve after peak load. However, the slope of the descending part of the curve after peak load represented the property of the crack propagation inside the specimen until failure (The failure after peak load is a relative issue depending to relative to the displacement at peak load). Fig. 10 indicated that the peak load values of SCGC specimens increased with an increase in replacement percentages of GGBFS that was attributed to the high strength of specimens when compared with control specimens (100% FA) accompanied

Table 6 Mechanical properties of SCGC

Mix code	Comp. Strength (MPa)	Splitting Tensile Strength (MPa)	Peak load (N)	Flexural strength (MPa)	Final disp.at mid span (mm)	Area under curve (N-mm)	Fracture Energy (N/m)	KIC (MPa-mm0.5)
S0SF0	24.25	1.58	1398.00	2.33	1.03	641.82	115.54	11.04
S25SF0	32.98	2.22	1661.00	2.77	1.02	664.40	118.71	13.11
S50SF0	40.10	3.50	2206.76	4.18	1.07	736.83	128.73	17.42
S75SF0	63.97	5.15	2607.82	4.35	1.10	882.63	152.38	20.59
S100SF0	76.19	6.45	2723.00	4.54	1.01	885.84	155.37	21.50
S0SF1	25.40	2.73	1785.70	2.98	9.44	4126.05	864.51	14.10
S25SF1	33.57	3.95	2170.00	3.62	8.97	4603.97	919.22	17.13
S50SF1	42.30	5.71	2548.00	4.25	8.50	4868.93	974.15	20.11
S75SF1	64.56	6.53	2870.65	4.78	8.14	5951.19	1150.79	22.66
S100SF1	77.14	8.26	3088.00	5.15	7.18	7001.43	1308.99	24.38

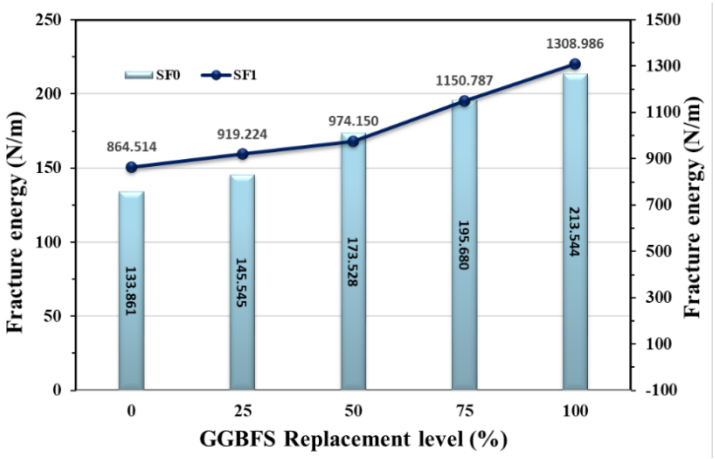

Fig. 11 Effect of GGBFS and SF replacement on fracture energy

by decreasing the values of displacement with an increase in GGBFS varience. The maximum increase/reduction (load/displacement) was achieved in specimens containing 100% GGBFS that exhibits maximum compressive strength value. In addition, incorporating SF results in a significant increase in the displacement value ranged between 0.5 mm to 9.5 mm for control specimens without SF (S0SF0) and the control specimens with SFs (S0SF1) respectively. However, the maximum peak load value is shown in the 100% replacement of GGBFS with SF (S100SF1).

The area under the load-displacement curve for each prismatic specimen was estimated and utilized in Eq. (2) to achieve the fracture energy (G_f) of each beam, and the final displacement at mid-span was recorded when the specimen failed. The results are shown in Table 6. The fracture energy for all mixes is represented in Fig. 11. It was detected that the fracture energy of SCGC specimens had increased as compared with control specimens. Generally, the fracture energy of SCGC inclined to increase with an increase in compressive strength, as shown in Fig. 11. Sarker and Ramgolam (2013) and Midhun *et al*. (2018) investigated that the fracture energy improved

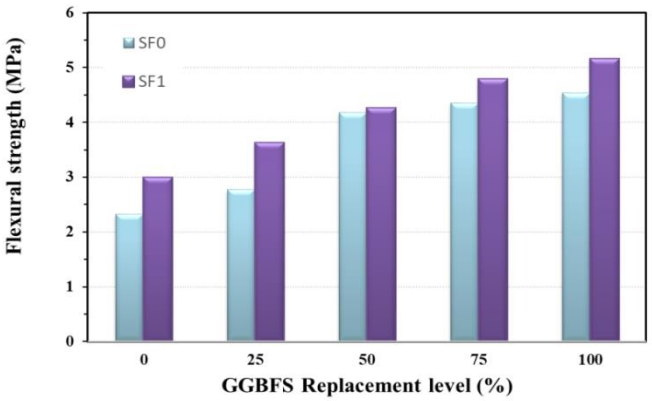

Fig. 12 Effect of GGBFS and SF replacement on flexural strength

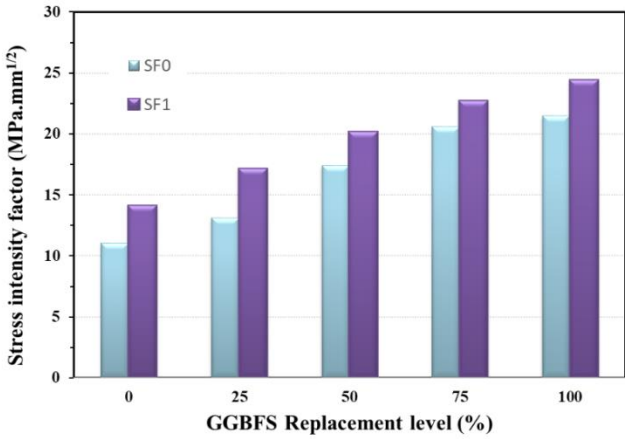

Fig. 13 Effect of GGBFS and SF replacement on stress intensity factor (KIC)

with the increase in compressive strength for heat-cured FA-based geopolymer concrete. Furthermore, the addition of SFs significantly increased the fracture toughness due to the crack propagation performance of SFs (Ganesan and Santhakumar 2013). However, the combination of SFs and GGBFS exhibit a superior effect on the fracture performance of SCGC.

The net flexural strength and critical stress intensity factor (KIC) of SCGC at 28 days were estimated by Eqs. (3) and (4) respectively, and represented in Figs. 12 and 13 respectively, and summarized in Table 6. The stress intensity factor refers to the amount of stress concentration near the crack tip when the crack starts to propagate. Similar to the aforementioned mechanical performance of SCGC, incorporating GGBFS had a superior effect on flexural strength and stress intensity factor values. In addition, the significant increase for both flexural and stress intensity factors were observed in the combination of SF with GGBFS.

3.3 Correlation between the fresh and hardened properties of SCGC:

The correlation of the experimental data can be conceder one of the most widespread applies among the researchers to evaluate the results were obtained. Theoretically, the relative volume

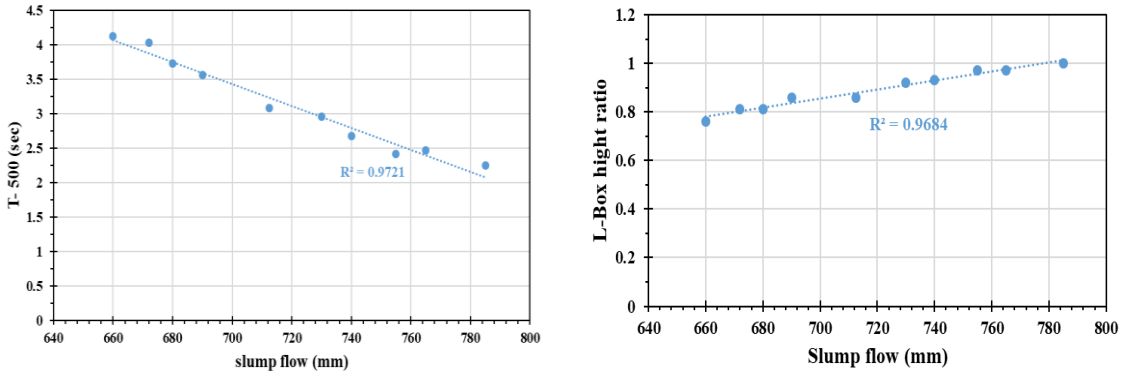

(a) Slump flow vs *T*-500 (b) Slump flow vs *L*-Box

Fig. 14 Relationship between the fresh properties of SCGC

fractions of the cementitious binder and aggregate are the major fundamentals that regulate the fresh and hardened properties of concrete. As shown previously, the higher compressive strength reflects the enhanced mechanical behavior.(Arabi *et al*. 2015, Abdullah *et al*. 2011) shown that the behavior of GPC is very similar to OPC. In order to estimate the relations among the properties of SCGC, the following correlation was found:

3.3.1 Correlation between the fresh properties of SCGC

Good relationships were found between the fresh properties of SCGC mixtures. The R^2 for the relationship between slump flow and *T*-500 flow, and *L*-Box was (R^2: 0.9721) and (R^2:0.9684) are shown in Fig. 14. The high value of (R^2), the coefficient of determination, specified that the slump flow and the other two properties were well correlated, despite the use of GGBFSs and/or SFs. This finding indicated the strong relationship between the fresh properties of SCGC in the study.

3.3.2 Correlation between the hardened properties of SCGC

The compressive strength values of FA-based SCGC with variance replacement of GGBFS and SF was found to exhibit similar performance to that of OPC concrete. In general, as the compressive strength increased, this resulted in a similar relative increase in terms of the values mechanical properties. It was observed from the results of compressive strength and other mechanical properties of SCGC that the incorporation of GGBFS with and without SF significantly increased the mechanical properties of SCGC. Additionally, the improved performance for all mechanical properties was observed having a similar trend.

An excellent relationship was found between the compressive strength and the other mechanical performance, as shown in Fig. 15. The value of (R^2) obtained from the relation between experimental compressive strength and splitting tensile strength with the theoretical values of the stress intensity factor (K_{IC}) and the net flexural obtained from different equations was the same. Therefore, it can be concluded that both equations are closed to each other, in addition to the experimental results.

3.4 Statistical evaluation of the test result

A general linear model analysis of variance (GLM-ANOVA) was performed at a significant

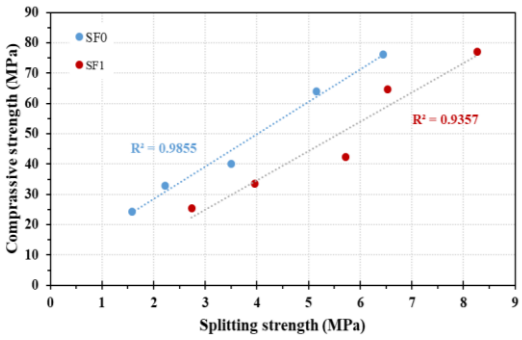

(a) Compressive vs splitting tensile strength

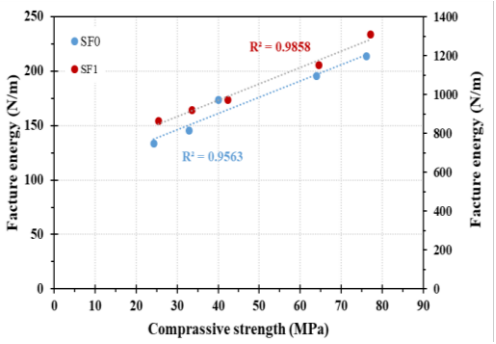

(b) Compressive vs fracture energy

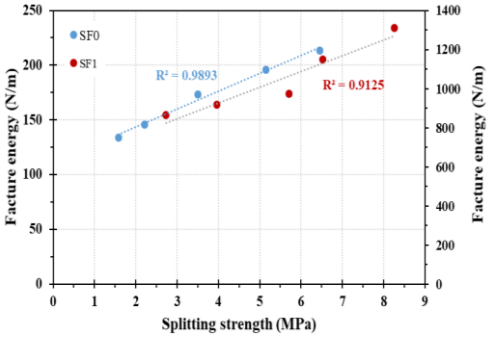

(c) Splitting tensile vs fracture energy

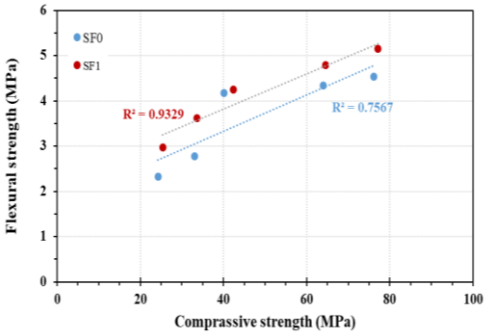

(d) Compressive vs flexural strength

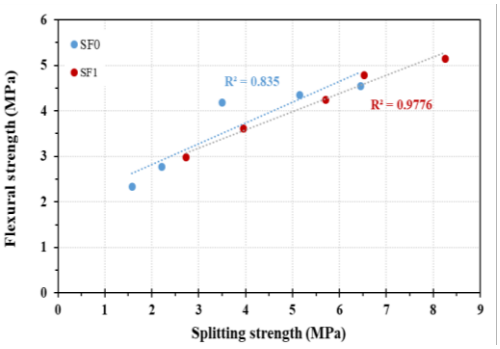

(e) Splitting tensile vs flexural strength

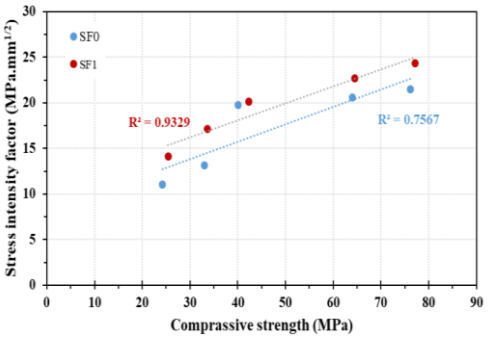

(f) Ccompressive vs stress intensity factor

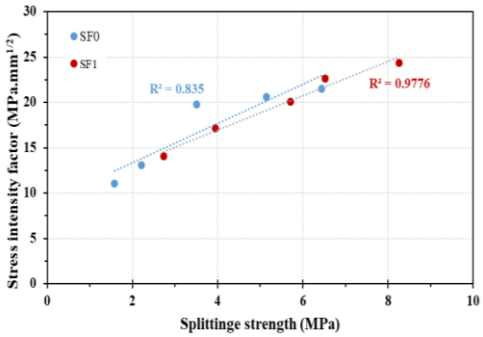

(g) Splitting tensile vs stress intensity factor

Fig. 15 The relationship between the hardened properties of SCGC

Table 7 Statistical evaluation of the test result

Dependent Variable	Independent variable	Sequential Sum of Squares	Mean Square	Computed *F*	*P* Value	significant
Slump flow diameter	Addition of SF	893.0	893.02	24.70	0.008	Yes
	GGBFS replacement level	15386.6	3846.65	106.41	0.000	Yes
	Error	144.6	36.15			
	Total	16424.2				
Slump flow time (T_{50})	Addition of SF	0.05625	0.05625	52.33	0.002	Yes
	GGBFS replacement level	4.23674	1.05918	985.29	0.000	Yes
	Error	0.00430	0.00107			
	Total	4.29729				
V-funnel flow time	Addition of SF	2.079	2.0794	28.57	0.006	Yes
	GGBFS replacement level	128.591	32.1478	441.68	0.000	Yes
	Error	0.291	0.0728			
	Total	130.962				
L-Box height ratio	Addition of SF	0.005290	0.005290	81.38	0.001	Yes
	GGBFS replacement level	0.053340	0.013335	205.15	0.000	Yes
	Error	0.000260	0.000065			
	Total	0.058890				
Compressive strength	Addition of SF	3.00	3.003	13.72	0.021	Yes
	GGBFS replacement level	3772.58	943.146	4307.66	0.000	Yes
	Error	0.88	0.219			
	Total	3776.46				
Splitting strength	Addition of SF	6.6647	6.66470	72.69	0.001	Yes
	GGBFS replacement level	34.7366	8.68416	94.72	0.000	Yes
	Error	0.3667	0.09168			
	Total	41.7681				
Flexural energy	Addition of SF	3329038	3329038	37.51	0.004	Yes
	GGBFS replacement level	370204	92551	1.04	0.484	No
	Error	355023	88756			
	Total	4054264				
Critical stress intensity factor	Addition of SF	15.259	15.2591	15.85	0.016	Yes
	GGBFS replacement level	156.321	39.0803	40.60	0.002	Yes
	Error	3.850	0.9625			
	Total	175.431				

level of 0.05 in order to estimate the variation in the tested performance of the SCGC with different level of GGBFS and/or SF in a quantitative form. For this, slump flow diameter, slump flow time (T50), *V*-funnel flow time, *L*-Box height ratio, compressive strength, splitting strength, flexural strength, and the critical stress intensity factor of the concretes were assigned as the dependent variables while the addition of the SFs and replacement level of GGBFS were the

factors. A statistical analysis was conducted to indicate the statistically significant factors (*p*-level <0.05). Table 7 presents the contributions of the factors on the evaluated test results. The column below the percent contribution offers an intention about the effect of the independent factors on the evaluated response, for example, the higher the contribution, the higher efficiency of the factors on that specific response. Also, the low influence of the factors on that specific response will be observed if the percent contribution is low. It was indicated by the results in Table 5 that all of the independent variables had a significant influence on the fresh and mechanical properties of SCGC.

When detecting the contribution amounts of the factors, it was observed that the most effective parameter in a variation of the fresh and hardened properties of the SCGC is GGBFS replacement level. The addition of SF had very little influence on the fresh properties and compressive strength as it was shown from the experimental results. However, the addition of SFs was indicated to be the most dominant factor in splitting tensile strength, flexural strength, stress intensity factor and fracture toughness of the SCGC. In addition, the combination of both GGBFS and SF was observed to be most impactful factor on all of the mechanical properties of SCGC.

4. Conclusions

Based on the experimental results, the following conclusions have been made on how GGBFS replacement and the addition of SF on the fresh and hardened properties of FA-based SCGCs can affect it. The conclusions are as follows;

- The fresh properties of SCGC are significantly affected by the GGBFS replacement level. Increasing the amount level of GGBFS on the mixes had a negative effect on the fresh properties. However, the addition of SF had a significant effect on the fresh properties of SCGC but still within the accepted range according to EFNARC.
- It can be deducted from the interaction of *V*-funnel flow and slump flow times that all of the SCGCs mixtures belonged to the boundaries of the viscosity class (VS2/VF2) as defined by the EFNARC. In addition, it was emphasized that such concrete might be helpful in improving segregation resistance or limiting the formwork pressure.
- It was indicated that the FA based SCGC had to be removed from the moulds two or three days after they were cast since they failed to get the target hardened after one day due to the low amount of CaO in FA which is the main factor affecting the initial setting time of concrete. However, this problem can be avoided by incorporating GGBFS in FA based geopolymer concrete.
- The FA based SCGC exhibited low compressive strength due to the low calcium content and low activity of FA. In addition, using of GGBFS in the mixes of SCGC significantly improved the compressive strength, since the amount of enhancement reaches up to more than 200% for the (S100SF0) specimens. This result showed the significant effect of GGBFS on the compressive strength values of SCGCs mixtures.
- As mentioned in earlier studies, the addition of SF on OPC concrete had a slight effect on the compressive strength values, however, it was indicated that the addition of SF had no significant effect on the compressive strength of SCGC.
- It was indicated that splitting tensile strength, flexural strength, fracture toughness, and stress intensity factor values were increased with an increase in the compressive strength and also improved with an increase in GGBFS contents compared to the control mix (100% FA). Furthermore, the combination of GGBFS replacement level with the addition of 1% of the SF

volume results in a superior increase in the mechanical performance of SCGC compared to the control mix without SFs (S0SF0).

• GGBFS replacement levels improved the mechanical properties of SCGC which resulted in a minimum load displacement and high peak load since the ductility of the concrete decreased with an increase in compressive strength. In addition, the incorporation of SF had a superior effect on the load-displacement values even for the specimens containing 100% GGBFS.

• The statistical analysis showed that all of the independent variables had a significant influence on the fresh and mechanical properties of SCGC and the most effective parameter in a variation of the fresh and hardened properties of the SCGC is GGBFS replacement level. In addition, the incorporation of SF had very little influence on the fresh properties and compressive strength. However, the addition of SFs proved to the most dominant factor in splitting tensile strength, flexural strength, stress intensity factor and fracture toughness of the SCGC. Moreover, the combination of both GGBFS and SF was observed to be most impact factor on all of the mechanical properties of SCGC.

• The main objective of this article is to study the behavior of GGBFS in this type of concrete with heat curing after positive behavior has been shown and for future study when GGBFS was added to the matrix at ambient temperatures curing due to present of high amount of reactive calcium silicate hydrates that form in conjunction with the geopolymeric gel.

References

Abdullah, M.M.A., Hussin, K., Bnhussain, M., Ismail, K.N. and Ibrahim, W.M.W. (2011), "Mechanism and chemical reaction of fly ash geopolymer cement-a review", *Int. J. Pure Appl. Sci. Technol*, **6**(1), 35-44.

Akcay, B. and Tasdemir, M.A. (2009), "Optimisation of using lightweight aggregates in mitigating autogenous deformation of concrete", *Constr. Build. Mater.*, **23**(1), 353-363.

Arabi, N., Chelghoum, N., Jauberthie, R. and Molez, L. (2015), "Formation of CSH in calcium hydroxide–blast furnace slag-quartz-water system in autoclaving conditions", *Adv. Cement Res.*, **27**(3), 153-62.

Arvaniti, E.C., Juenger, M.C., Bernal, S.A., Duchesne, J., Courard, L., Leroy, S., ... and De Belie, N. (2015), "Determination of particle size, surface area, and shape of supplementary cementitious materials by different techniques", *Mater. Struct.*, **48**(11), 3687-3701.

ASTM (2010), ASTM C127-10 Standard Test Method for Density, Relative Density (Specific Gravity), and Absorption of Coarse Aggregate, ASTM International, 1-6.

ASTM, C496 (2001), Standard Test Method for Splitting Tensile Strength of Cylindrical Concrete Specimens, Annual Book of American Society of Testing and Materials, 2-4.

ASTM, C39 (2001), 39, Standard Test Method for Compressive Strength of Cylindrical Concrete Specimens, ASTM International.

Belkowitz, J.S., Belkowitz, W.B., Nawrocki, K. and Fisher, F.T. (2015), "Impact of nanosilica size and surface area on concrete properties", *ACI Mater. J.*, **112**(3), 419-427.

Çevik, A., Alzeebaree, R., Humur, G., Niş, A. and Gülşan, M.E. (2018), "Effect of nano-silica on the chemical durability and mechanical performance of fly ash based geopolymer concrete", *Ceram. Int.*, **44**(11), 12253-12264.

Chi, M. and Huang, R. (2013), "Binding mechanism and properties of alkali-activated fly ash/slag mortar", *Constr. Build. Mater.*, **40**, 291-298..

Corinaldesi, V. and Moriconi, G. (2011), "Characterization of self-compacting concretes prepared with different fibers and mineral additions", *Cement Concrete Compos.*, **33**(5), 596-601.

Davidovits, J. (1993), "Geopolymer cement to minimize carbon-dioxde Greenhouse-Warming", *Ceram. Trans.*, **37**, 165-182.

Davidovits, J. (2008), *Geopolymer Chemistry and Applications*, 2nd Edition, Institut Geopolymer, SaintQuentin, France.
Davidovits, J. (1991), "Geopolymers: inorganic polymeric new materials", *J. Therm. Anal. Calorimet.*, **37**(8), 1633-1656.
Dombrowski, K., Buchwald, A. and Weil, M. (2007), "The influence of calcium content on the structure and thermal performance of fly ash based geopolymers", *J. Mater. Sci.*, **42**(9), 3033-3043.
Dubey, R. and Kumar, P. (2012), "Effect of superplasticizer dosages on compressive strength of self compacting concrete", *Int. J. Civil Struct. Eng.*, **3**(2), 360-366.
Duxson, P., Fernández-Jiménez, A., Provis, J.L., Lukey, G.C., Palomo, A. and van Deventer, J.S. (2007), "Geopolymer technology: the current state of the art", *J. Mater. Sci.*, 42(9), 2917-2933.
EFNARC (2005), The European Guidelines for Self-Compacting Concrete: Specification, Production and Use, The European Guidelines for Self Compacting Concrete, no. May.
Ersatz (1990), "Eurocode: grundlagen der tragwerksplanung;\nDeutsche fassung EN 1990:2002 + A1:2005 + A1:2005/AC:2010\n", A1 Berichtigung, **1**, 2002-102010.
Frazão, C., Camões, A., Barros, J. and Gonçalves, D. (2015), "Durability of steel fiber reinforced self-compacting concrete", *Constr. Build. Mater.*, **80**, 155-166.
Ganesan, N., Indira, P.V. and Santhakumar, A. (2013), "Engineering properties of steel fibre reinforced geopolymer concrete", *Adv. Concrete Constr.*, **1**(4), 305-318.
Gencel, O., Brostow, W., Datashvili, T. and Thedford, M. (2011), "Workability and mechanical performance of steel fiber-reinforced self-compacting concrete with fly ash", *Compos. Interf.*, **18**(2), 169-184.
Hardjito, D. and Rangan, B.V. (2005), "Development and properties of low-calcium fly ash-based geopolymer concrete", Research Report GC 1, Faculty of Engineering, Curtin University of Technology, Perth, Australia
Hardjito, D., Wallah, S.E., Sumajouw, D.M. and Rangan, B.V. (2004), "On the development of fly ash-based geopolymer concrete", *Mater. J.*, **101**(6), 467-472.
Iqbal, S., Ali, A., Holschemacher, K. and Bier, T.A. (2015), "Effect of change in micro steel fiber content on properties of High strength Steel fiber reinforced Lightweight Self-Compacting Concrete (HSLSCC)", *Procedia Eng.*, **122**, 88-94.
Jindal, B.B., Singhal, D. and Sharma, S.K. (2017), "Improving compressive strength of low calcium fly ash geopolymer concrete with alccofine", *Adv. Concrete Constr.*, **5**(1), 17-29.
Khaloo, A., Raisi, E.M., Hosseini, P. and Tahsiri, H. (2014), "Mechanical performance of self-compacting concrete reinforced with steel fibers", *Constr. Build. Mater.*, **51**, 179-186.
Kong, D.L. and Sanjayan, J.G. (2008), "Damage behavior of geopolymer composites exposed to elevated temperatures", *Cement Concrete Compos.*, **30**(10), 986-991.
Gülşan, M.E., Mohammedameen, A., Şahmaran, M., Niş, A., Alzeebaree, R. and Abdulkadir, Ç. (2018), "Effects of sulphuric acid on mechanical and durability properties of ECC confined by FRP fabrics", *Adv. Concrete Constr.*. **6**(2), 199-220.
Memon, F.A, Nuruddin, F. and Shafiq, N. (2011), "Compressive strength and workability characteristics of low-calcium fly ash-based self-compacting geopolymer concrete", *Int. J. Civil Environ. Eng.*, **3**(2), 72-78.
Memon, F.A., Nuruddin, M.F., Demie, S. and Shafiq, N. (2011), "Effect of curing conditions on strength of fly ash-based self-compacting geopolymer concrete", *Int. J. Civil Environ. Eng.*, **3**, 183-86.
Midhun, M.S., Gunneswara Rao, T.D. and Chaitanya Srikrishna, T. (2018), "Mechanical and fracture properties of glass fiber reinforced geopolymer concrete", *Adv. Concrete Constr.*, **6**, 29-45.
Noushini, A. and Castel, A. (2016), "The effect of heat-curing on transport properties of low-calcium fly ash-based geopolymer concrete", *Constr. Build. Mater.*, **112**, 464-477.
Nuruddin, F., Demie, S., Memon, F.A. and Shafiq, N. (2011), "Effect of superplasticizer and NaOH molarity on workability, compressive strength and microstructure properties of self-compacting geopolymer concret", *World Acad. Sci., Eng. Technol.*, **74**(3), 8-14.
Peterson, P.E. (1980), "Fracture energy of concrete: Method of determination", *Cement Concrete Res.*, **10**(1). 79-89.

Rangan, B.V. (2008), *Low-Calcium, Fly-Ash-Based Geopolymer Concrete*, Concrete Construction Engineering Handbook Taylor and Francis Group, Boca Raton, FL.

Recommendation, R.D. (1985), "Determination of the fracture energy of mortar and concrete by means of three-point bend tests on notched beams", *Mater. Struct.*, **18**(106), 285-290.

Sarker, P.K., Haque, R. and Ramgolam, K.V. (2013), "Fracture behaviour of heat cured fly ash based geopolymer concrete", *Mater. Des.*, **44**, 580-586.

Tamil Selvi, M. and Thandavamoorthy T.S. (2014), "Mechanical and durability properties of steel and polypropylene fibre reinforced concrete", *Int. J. Earth Sci. Eng.*, **7**(2), 696-703.

Temuujin, J., van Riessen, A. and MacKenzie, K.J.D. (2010), "Preparation and characterisation of fly ash based geopolymer mortars", *Constr. Build. Mater.*, **24**(10), 1906-1910.

CC